JACS
JOURNAL OF THE AMERICAN CHEMICAL SOCIETY
Article
pubs.acs.org/JACS

Extension of Light-Harvesting Ability of Photosynthetic Light-Harvesting Complex 2 (LH2) through Ultrafast Energy Transfer from Covalently Attached Artificial Chromophores

Yusuke Yoneda,[†] Tomoyasu Noji,[‡,§] Tetsuro Katayama,[∥,⊥] Naoto Mizutani,[‡] Daisuke Komori,[‡] Mamoru Nango,[‡,§] Hiroshi Miyasaka,[†] Shigeru Itoh,[#] Yutaka Nagasawa,*[,†,⊥,⊗] and Takehisa Dewa*[,‡,⊥]

[†]Graduate School of Engineering Science, Osaka University, Toyonaka, Osaka 560-8531, Japan

[‡]Department of Frontier Materials, Graduate School of Engineering, Nagoya Institute of Technology, Gokiso-cho, Showa-ku, Nagoya, Aichi 466-8555, Japan

[§]The OCU Advanced Research Institute for Natural Science & Technology (OCARINA), Osaka City University, 3-3-138 Sugimoto, Sumiyoshi-ku, Osaka 558-8585, Japan

[∥]Institute for NanoScience Design, Osaka University, Toyonaka, Osaka 560-8531, Japan

[⊥]PRESTO, Japan Science and Technology Agency (JST), Kawaguchi, Saitama 332-0012, Japan

[#]Center for Gene Research, Nagoya University, Furo-cho, Chikusa-ku, Nagoya, Aichi 464-8602, Japan

Supporting Information

ABSTRACT: Introducing appropriate artificial components into natural biological systems could enrich the original functionality. To expand the available wavelength range of photosynthetic bacterial light-harvesting complex 2 (LH2 from *Rhodopseudomonas acidophila* 10050), artificial fluorescent dye (Alexa Fluor 647: A647) was covalently attached to N- and C-terminal Lys residues in LH2 α-polypeptides with a molar ratio of A647/LH2 $\simeq$ 9/1. Fluorescence and transient absorption spectroscopies revealed that intracomplex energy transfer from A647 to intrinsic chromophores of LH2 (B850) occurs in a multiexponential manner, with time constants varying from 440 fs to 23 ps through direct and B800-mediated indirect pathways. Kinetic analyses suggested that B800 chromophores mediate faster energy transfer, and the mechanism was interpretable in terms of Förster theory. This study demonstrates that a simple attachment of external chromophores with a flexible linkage can enhance the light harvesting activity of LH2 without affecting inherent functions of energy transfer, and can achieve energy transfer in the subpicosecond range. Addition of external chromophores, thus, represents a useful methodology for construction of advanced hybrid light-harvesting systems that afford solar energy in the broad spectrum.

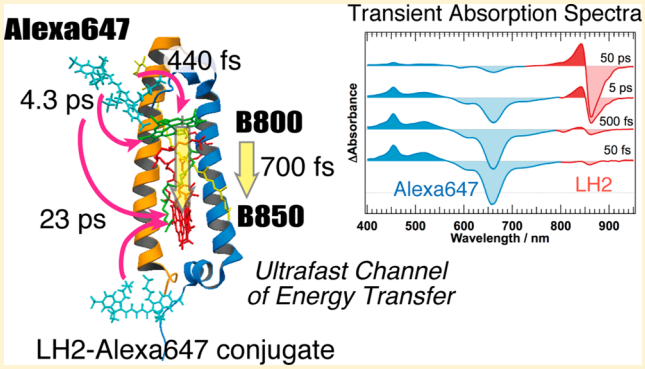

INTRODUCTION

Light-harvesting strategies are of crucial importance for the establishment of renewable energy production systems that can utilize solar energy with high efficiency. Studying photosynthetic systems and mimicking their highly efficient mechanisms can be a very important approach to develop artificial photosynthetic systems for solar-energy conversion. One way to accomplish this goal is the "bottom-up approach," with construction of a valid two- or three-dimensional molecular assembly starting at a single-molecule level.[1−3] Another approach is to introduce appropriate additional parts into the natural system so as to construct a hybrid system that enriches the original functionality.[4−11] Both approaches have advantages, but the latter can expand the original functions by simply attaching artificial molecules at appropriate positions. However, one has to consider influences of such modifications on the inherent functions.

Photosynthetic organisms have diverse light-harvesting antenna systems that have evolved to adapt to their habitats with different or variable intensities and colors of light.[12−14] Their light-harvesting complexes perform highly efficient photon capture followed by ultrafast excitation energy transfer between multiple chromophores.[14−18] Some purple photosynthetic bacteria have peripheral light-harvesting complex 2 (LH2), whose beautiful cylindrical structures have been revealed by X-ray crystallography.[19−21] LH2 from *Rhodopseudomonas acidophila* strain 10050 consists of nine-membered pairs of α, β-apoproteins and 27 bacteriochlorophyll *a* (BChl)

Received: August 12, 2015
Published: September 24, 2015

DOI: 10.1021/jacs.5b08508
J. Am. Chem. Soc. 2015, 137, 13121−13129

and 9 carotenoids (rhodopin glucoside).[19,21] BChl molecules form two types of characteristic assemblies, B800 and B850, named according to their absorption peak wavelengths. It is well-known that light energy absorbed by B800 is transferred to B850 with a time constant of ∼700 fs.[22,23] Light energy absorbed by carotenoids is also efficiently transferred to B800 and B850.[24−26] Consequently, the light energy is rapidly and efficiently collected by B850 in a subpicosecond time domain. The excitation energy on B850 is then transferred to B850 of neighboring LH2 complexes, and finally funneled into a core complex composed of light-harvesting 1 antenna and reaction center complexes (LH1-RC), where charge separation follows.[27−30] LH2 and LH1-RC, therefore, form a highly efficient fused excitonic and photovoltaic device.

LH2 possesses absorption bands in the visible and near-infrared regions because of the intrinsic chromophores, and exhibits low absorbance in the range of 620−750 nm. Recent studies have demonstrated that external fluorescent dyes enhance absorption cross sections of reconstituted LH1 (B820- and B875-type),[4−6] and increase the charge-separation capacity of reaction center complexes.[8−11] Energy transfer from fluorescent dyes to intrinsic BChl molecules in the reconstituted LH1-type complexes took place efficiently (>90%) in the broad time domain of a few to hundreds of picoseconds, presumably by the Förster-type mechanism.[4−6] This strategy using LH1-polypeptides as building blocks, which binds external chromophores with defined positions, has provided a potential strategy to assemble energy transfer cascade using multiple chromophores with high efficiency.

Compared to LH1-type complex, B850 assembly in LH2 is robust and possesses the higher output energy, which is collected from B800 and carotenoids. Previous works demonstrated that B800 BChls in LH2 can be substituted with other chlorophyll derivatives.[31−33] The energy transfer from the replaced chromophores in the B800 position to B850 occurred in the time domain of 0.8−8.3 ps.[32] The short time constant, however, is ∼5 times shorter than predicted by simulations according to a Förster-type mechanism with the spectral overlap.[34] Therefore, the Q_y absorption of B850, which exhibits a very broad absorption band beyond 14,500 cm^{-1} (∼690 nm) due to contribution from the higher excitonic bands,[35,36] appears to serve as the energy accepting band in the ultrafast time domain.

In this study, we constructed LH2 that covalently attaches artificial fluorophores (Alexa Fluor 647: A647) as an auxiliary light-harvesting pigment to extend the light-harvesting activity without affecting inherent functions. Ultrafast spectroscopy was carried out and energy transfer from A647 to B850 manifold was found to occur in a multiexponential manner in the time range of subpicoseconds to tens of picoseconds. Kinetic analyses clearly characterized the pathways of energy transfer in the time domain. Interestingly, the ultrafast energy transfer can be achieved through the inherent ultrafast channel, B800 → B850. To our knowledge, the subpicosecond energy transfer is the fastest among the hybrid photosynthetic antenna systems ever constructed.[4−6] Furthermore, the final B850 exciton bears a lifetime of 1.2 ns, which is long enough for it to be efficiently utilized by subsequent energy conversion processes.

RESULTS AND DISCUSSION

Conjugation of A647 to LH2. A647-maleimide fluorophore was attached to Lys residues of LH2 polypeptides via a bifunctional cross-linker reagent, sulfosuccinimidyl 6-[3′-(2-pyridyldithio)propionamido]hexanoate (sulfo-LC-SPDP). There are three Lys residues in LH2 α- and one in β-polypeptides. Amino acid sequences were shown in Figure 1. Sodium dodecyl sulfate polyacrylamide gel electrophoresis (SDS−PAGE) indicated that A647 was attached to LH2 α-polypeptides selectively (Figure S1 in the Supporting Information). Judging from the absorption spectrum of the LH2−A647 conjugate (Figure 2A), 8.6 ± 0.5 of A647 molecules were attached to one LH2 complex, that is, A647/LH2 α-polypeptide ≃ 1/1 (mol/mol). MALDI-TOF-MS and ESI-MS/MS analyses were carried out to identify which Lys residues were modified with the PDP-linker moiety. Peptide fragments, whose either N-terminal (K5) or C-terminal (K50 or 51) region was modified with the PDP-linker moiety, were determined (Figure S2). Doubly modified α-polypeptide was not detected by the MS analyses. The X-ray crystallographic structure of LH2 obtained at 100 K revealed that K5 and K50 residues are hydrogen-bonded with rhodopin glucoside and His residue of neighboring LH2 β-polypeptide (H41), respectively.[21] At 4 °C these Lys residues are reactive for the modification. Therefore, only one of the three possible sites (K5, K50, and K51) was estimated to be modified. The MS analyses could not distinguish between K50- and K51-modification. Hereafter, the latter residue is regarded as the C-terminal-modified one for descriptive purposes. The K13 residue in β-polypeptide facing outward is unreactive, possibly because the reactivity of K13 located in the end of the hydrophobic core region of β-polypeptide is hindered by LDAO molecules bound to the region. The positions of these residues are indicated in Figure 1. As a result, the labeling

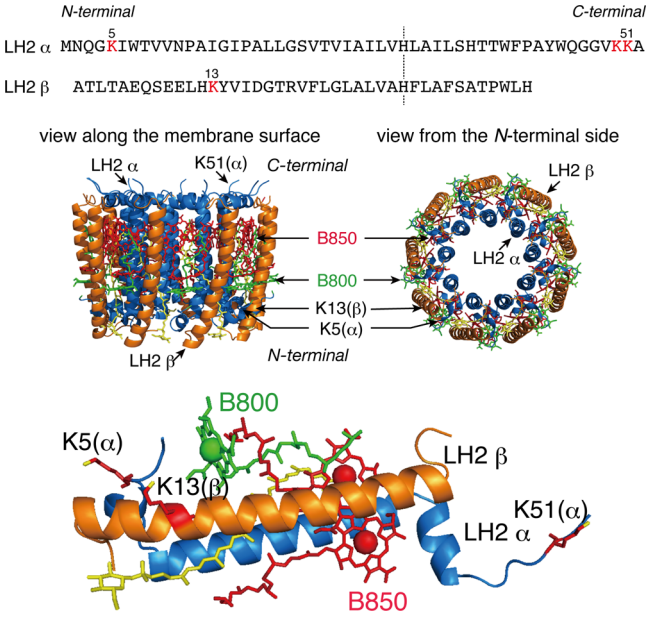

Figure 1. Amino acid sequences of LH2 α- and β-polypeptides of *R. acidophila* strain 10050 (upper), and the crystallographic structure of LH2 (middle left, view along the membrane surface; right, view from the N-terminal side) and the subunit structure (bottom) composed of BChls (B800 and B850), rhodopin glucoside, α- and β-polypeptides. Histidine residues that ligate BChl forming B850 were indicated by a dotted vertical line, and all Lys residues in the sequences are colored in red in the scheme of amino acid sequence. The positions of K5 and K51 in α-polypeptide and K13 in β-polypeptide are indicated in the structural drawing. The subunit structure was depicted using PyMOL on the basis of the crystallographic structure 1NKZ.[21]

DOI: 10.1021/jacs.5b08508
J. Am. Chem. Soc. 2015, 137, 13121−13129

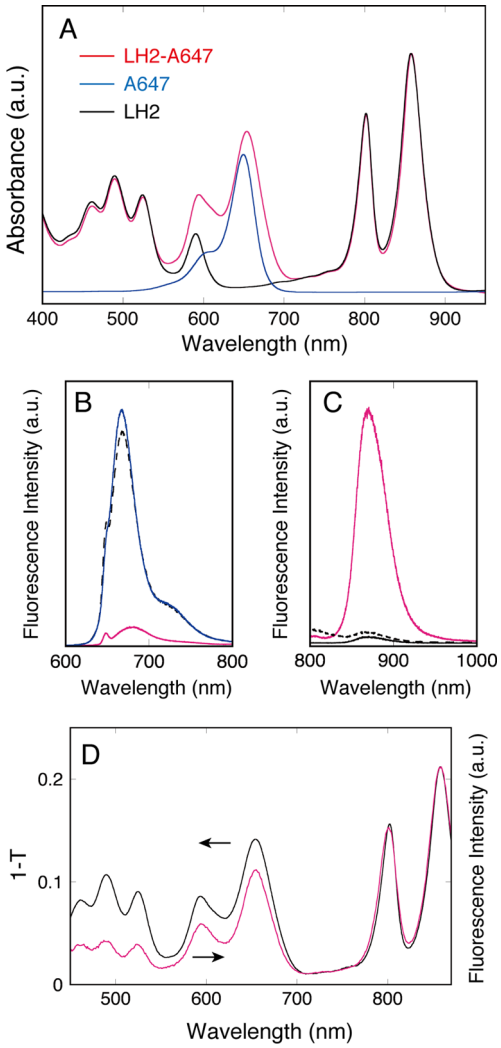

Figure 2. Static absorption, fluorescence, and excitation spectra of LH2−A647 dissolved in a Tris-HCl buffer (20 mM, pH 8.0, 0.1 wt % LDAO). Absorption (A) and fluorescence spectra (B and C) of LH2−A647 conjugate (solid red), LH2 (solid black), and A647 (solid blue). Dashed lines in B and C represent emission spectra of a simple mixture of A647 and LH2 at a molar ratio of ∼9/1. Excitation wavelength: 647 nm. Sample concentration was adjusted to OD = 0.1 at λ_{max} of A647 for panel B and that of B850 for LH2−A647 and LH2 in panel C. Excitation spectrum of LH2−A647 (red line) monitored at 880 nm was compared with absorptance (1 − T, T: transmittance) spectrum (black line), normalized at the maximum of B850 in panel D.

manner was established to be one A647 per α-polypeptide, either on the N-terminal K5 or C-terminal K51 (or K50).

Spectroscopic Properties of LH2−A647. Absorption spectrum of LH2−A647 is shown in Figure 2A. These absorption maxima and band shapes can be reproduced as a sum of A647 and intrinsic chromophores, BChl (B850 and B800) and rhodopin glucoside.[37] The absorption bands and CD signals (Figure S3) of the intrinsic chromophores in LH2 were well preserved, indicating that modification with A647 does not perturb the environment of the intrinsic chromophores. A647 exhibited a red shift of 5 nm in the absorption maximum (from 650 to 655 nm) in the conjugate, which is a solvatochromic shift probably due to the interaction with LH2, as indicated previously.[8] CD signals around 650 nm indicated no excitonic coupling between A647s (Figure S3). Linear dichroism spectra of LH2−A647 in a squeezed polyacrylamide gel medium suggested random orientation of A647 with respect to B800 and B850 BChl molecules (data not shown).

Figure 2B,C shows fluorescence spectra of the conjugate and the constituents excited at 647 nm. Compared to free A647 or a simple mixture of A647 and LH2, significant quenching of A647 fluorescence was observed in LH2−A647 (Figure 2B). Associated with the quenching of A647, there was pronounced emission from B850 at 868 nm in LH2−A647 (Figure 2C). These results indicate rapid energy transfer taking place from A647 to B850. Energy transfer efficiency, E, was estimated to be 89% from the equation, $E = 1 - F'/F$, where F' and F represent fluorescence intensities of A647 in the presence and the absence of the acceptor LH2, respectively. The excitation spectrum of LH2−A647 (Figure 2D) also indicated that the efficient energy transfer from A647 to B850 occurs with an efficiency of 83%. Energy transfer efficiency estimated from fluorescence lifetime was 86% (Figure S4) consistent with the steady-state fluorescence measurements. When free A647 was simply mixed with LH2 in solution, the fluorescence lifetime was identical to that of free A647 alone, indicating that only the ones covalently attached to LH2 contribute to the energy transfer.

Transient Absorption Spectroscopy. For the direct elucidation of the energy transfer dynamics, femtosecond transient absorption (TA) spectroscopy was applied with a laser pulse, with its spectrum centered at 650 nm to excite the absorption band of A647 in the conjugate (Figure S5). The femtosecond TA spectrum of LH2−A647 in Figure 3 shows

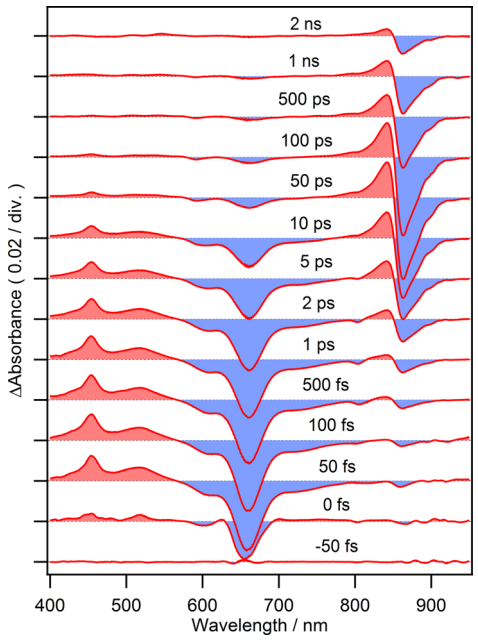

Figure 3. Transient absorption spectra of LH2−A647 excited at 650 nm with a pulse duration of ∼17 fs. The time delays are indicated in the figure.

that, immediately after the photoexcitation, a negative band with a minimum at 657 nm and positive bands with maxima at 517 and 454 nm appear within the response time of the apparatus. The negative band is safely ascribed to the superposition of ground state bleach (GSB) and stimulated emission (SE) of A647, and the positive bands to the excited state absorption of A647 in comparison with the TA spectrum

DOI: 10.1021/jacs.5b08508
J. Am. Chem. Soc. 2015, 137, 13121−13129

of free A647 in a buffer solution (Figure S6). The lifetime of the excited state of free A647 was ~1.2 ns, which agrees with the fluorescence lifetime of 1.17 ns measured by a streak-camera system (Figure S4). Recently, Dutta et al. reported biexponential decay of A647 in Tris-HCl buffer solution with lifetimes of 0.41 ns (6.9%) and 1.09 ns (93.1%),[8] with the latter corresponding to the natural fluorescence lifetime. Although the origin of the former component is unknown, the absence of the component in our present sample could be attributed to LDAO in the solution, providing a more homogeneous environment for A647.

With the increase in the delay time after the excitation, the signal due to the A647 moiety decays in the picosecond time domain with simultaneous appearance of new positive and negative bands at 842 and 863 nm, which are ascribed to the exciton absorption and the superposition of GSB and SE of B850, respectively.[38] To elucidate the dynamics, we applied global analysis to the time dependence of the differential absorbance (Δ_{abs}) at various wavelengths and some of the results are shown in Figure 4. Filled circles represent the time

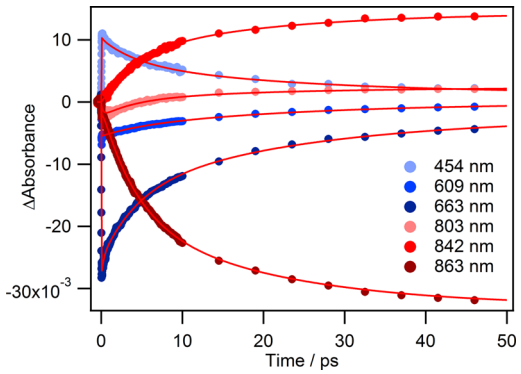

Figure 4. Time dependence of the Δ_{abs} at six different wavelengths indicated in the figure (filled circles) and the result of global analysis fitting (solid curves).

dependent signal changes and the solid curves are the results of the analysis. The time evolution can be better reproduced with four components, rather than three. The four-component analysis of decay-associated spectra (DAS) with time constants of 260 fs, 4.3 ps, 23 ps, and 1.2 ns is depicted in Figure 5. Positive and negative bands in DAS represent decrease and increase in Δ_{abs}. For the negative band at 650–660 nm, the amplitude ratio for the corresponding time constants ($a/b/c/d$) was 0.14:0.35:0.42:0.09, respectively.

The strong positive and negative bands at 842 and 863 nm, respectively, with the longest time constant of 1.2 ns (Figure 5d), were a result of the B850 exciton.[39,40] Weak positive and negative bands at 400–580 and 580–720 nm, respectively, were due to the conjugated A647, which is not involved in the energy transfer and accounts for 9% of the total excited state of A647 (A647*). The lifetime of A647* coincidently matches with that of the B850 exciton, although no specific interaction was detected between them. This result is consistent with the observation in the fluorescence decay of LH2–A647, where 8% of the conjugated A647 had a long lifetime of 1.37 ns and was not involved in the energy transfer (Figure S4).

For the DAS with lifetimes of 4.3 and 23 ps (Figure 5b,c), a negative band appears at 660 nm, indicating a decrease of the A647*, while negative and positive bands appear at 842 and 863 nm, respectively. This result clearly indicates the

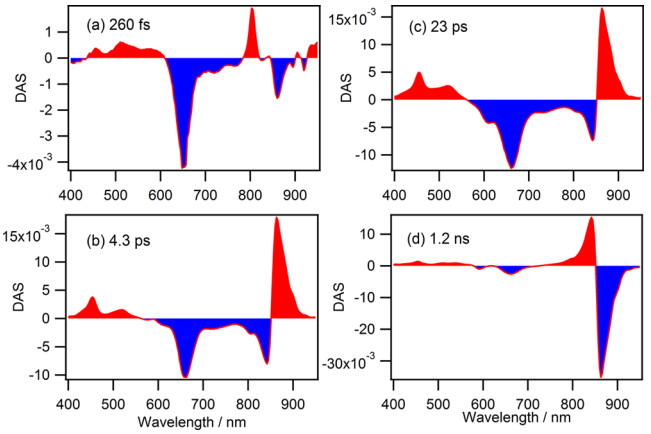

Figure 5. Decay associated spectra (DAS) obtained from the global analysis of the TA spectra of LH2–A647: components with time constants of (a) 260 fs, (b) 4.3 ps, (c) 23 ps, and (d) 1.2 ns were obtained.

appearance of B850 exciton by the energy transfer from the conjugated A647. The fast and slow time constants for the energy transfer may reflect different locations of the conjugated A647, i.e., those at N- and C-terminal regions exhibit different rate of energy transfer. The details will be discussed in the later sections.

The DAS with a lifetime of 260 fs (Figure 5a) showed a negative peak at 650 nm, whereas the DAS with longer lifetimes (Figures 5b–d) showed a peak at 660 nm. The 260 fs negative band thus indicates the red-shift of the SE of A647 by structural relaxation or solvation. However, positive and negative bands at 803 and 860 nm, respectively, in Figure 5a also indicate the energy transfer to B800 or B850. Close inspection of the TA spectra of LH2–A647 at 0.5, 1.0, and 2.0 ps in Figure 3 indicates a small negative band at 803 nm. The time dependence of Δ_{abs} at 800 nm in Figure 6a clearly exhibits appearance and disappearance of the negative band with time

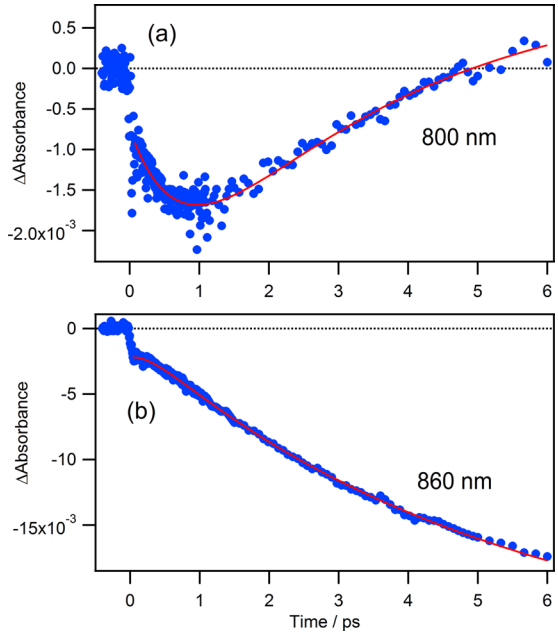

Figure 6. Time dependence of the Δ_{abs} at (a) 800 nm and at (b) 860 nm (blue filled circles) with the fitting curve (red solid curves).

DOI: 10.1021/jacs.5b08508
J. Am. Chem. Soc. 2015, 137, 13121–13129

constants of 840 ± 140 fs (0.47) and 2.1 ± 0.4 ps (−0.53), respectively. The time constant of 840 fs is significantly slower than that for the internal conversion from the directly excited Q_x state of BChl.[41] In the Δ_{abs} trace at 860 nm, shown in Figure 6b, a small negative signal appears immediately at the time origin within the instrumental response time, due to the direct excitation at Q_x band of B850, which was unclear for B800 at 800 nm. A delay for a few hundreds of femtoseconds was detected before the subsequent increase of the negative band. The time-evolution of Δ_{abs} at 860 nm can be fitted by two positive components with time constants of 3.8 ± 0.1 ps (0.43) and 19 ± 1 ps (0.52) and a small negative component with a time constant of 280 ± 30 fs (−0.05). These results indicate that the energy transfer partially occurs through the excited state of B800 (B800*), i.e., A647 → B800 → B850. The A647 attached at the K5 position, which is closer to B800, is likely to contribute to this pathway. In the B800-removed LH2−A647, the transfer efficiency was only 54−75% (data not shown), suggesting the B800 contributes to the energy transfer in some extent.

TA Measurements for Intrinsic Energy Transfer in LH2. Some portion of BChls could have been directly excited at the Q_x band centered at 594 nm because of the wide bandwidth (~90 nm) of the excitation spectrum centered at 650 nm. The excitation would lead to an ultrafast internal conversion to the lowest exciton state with a time constant of ~50 fs,[41] which may alter the result of the present experiment. To clearly elucidate the ultrafast channel of the energy transfer from A647, the TA spectrum was measured for LH2 with the excitation at 600 nm (Figure S7). The negative band at 860 nm, which corresponds to the superposition of GSB and SE of B850, appears immediately within the instrumental response time and subsequently continues to deepen with a time constant of 620 ± 80 fs. This result indicates that Q_x bands of both B800 and B850 are excited by the 600 nm laser pulse and the intensity ratio of the immediate (directly excited B850) and slower component (energy transfer from B800 to B850) is about 3:1. The negative B850 band is nearly five times shallower than that of LH2−A647 measured upon the excitation at 650 nm, even though similar pulse energy of 10.5 nJ was applied for both excitations. When the Δ_{abs} is compared at 860 nm at the time origin (ca. -2.2×10^{-3}) and 62 ps (ca. -3.2×10^{-2}) for LH2−A647 (Figure 6b), the ratio of directly excited B850 is estimated to be only ~0.07 of the total excited B850 produced. These results confirm that direct excitation at the Q_x band is minor in the case of 650 nm excited LH2−A647. Thus, the observed dynamics can be attributed to the energy transfer process from conjugated A647 to BChls of LH2.

We also directly excited the $S_2 \leftarrow S_0$ transition of carotenoid in LH2−A647 conjugate with laser pulses centered at 514 nm. Immediately after the excitation, GSB with a clear vibrational structure at 400−550 nm and SE at 550−680 nm appeared (Figure S8). After 500 fs, the SE was taken over by a TA band that peaks at 578 nm, which is assigned to the S_1 state of the carotenoid.[26,42] Simultaneously, in the picosecond domain, the TA band was taken over by the bands due to B850. The multiexponential fitting of the time evolution of the Δ_{abs} at 578 nm resulted in rise times of 51 ± 4 fs (0.76) and 280 ± 20 fs (0.24), and a decay time of 3.8 ± 0.1 ps. The band at 578 nm does not appear when A647 moiety is excited, indicating that the S_1 state of carotenoid[26] is not involved in the A647 → B850 energy transfer pathway.

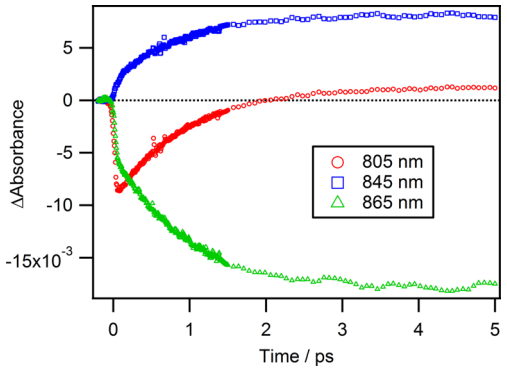

Figure 7. Time dependence of the Δ_{abs} at 805, 845, 865 nm upon excitation at 775 nm for LH2−A647. Also see Figure S9 for detailed information.

The energy transfer from B800 to B850 is reported to occur with a time constant of 0.6−0.8 ps.[22,23] This process was also observed for LH2−A647 with excitation at 775 nm as shown in Figure 7 (also see Figure S9 with TA spectra and DAS). The negative TA at 800 nm decays with a time constant of 0.89 ± 0.01 ps, as seen in intact LH2, suggesting that the modification of LH2 with A647 does not influence the intrinsic B800 → B850 energy transfer. Unity efficiency of the energy transfer in LH2−A647 was well conserved as seen in the fluorescence excitation spectrum that completely overlap with the absorptance spectrum in the B800 band (Figure 2D). As this process occurs in the subpicosecond domain, the B800* would not be populated as much as an intermediate state in the A647 → B850 energy transfer, as seen in Figures 3, 5, and 6a.

Energy Transfer Kinetics. The current experimental results depict the energy transfer in LH2−A647 as follows: (a) about 10% of the A647s do not exhibit energy transfer to the LH2 within the excited state lifetime of 1.2 ns, (b) energy transfer between A647s is absent because excitation energy dependence on the TA spectra indicated no singlet−singlet annihilation between A647s (see the discussion in the Supporting Information regarding the annihilation, and Figures S10 and S11), and (c) energy transfer occurs either directly from A647 to B850, or via B800 to B850. The femtosecond TA measurements indicate that the rate of energy transfer via B800 is faster than that of direct transfer from A647 to B850. Thus, the component with the time constant of 260 fs presumably involve not only structural relaxation and/or ultrafast solvation of A647* but also energy transfer by way of B800 to B850. The 4.3 ps component can be assignable to this pathway, although the possibility that this component could also involve the direct pathway, A647 → B850, cannot be ruled out. The time constant of 23 ps is safely ascribed to the direct energy transfer of A647 → B850. When the positions of A647s attached to LH2 α-polypeptides are considered, those attached to N- and C-terminal regions, where B800 and B850 are much closer, should be responsible for the faster and the slower transfer pathways, respectively. The origin of 1.2 ns component is unclear at this moment. Free A647s in the solution could be a possibility, although it was not detected by the SDS-PAGE analysis. A647 fixed in unfavorable positions and orientations for energy transfer could be another possibility. In any case, we included the component in the kinetic analysis without making any speculation.

The model energy transfer diagram according to these observations is represented in Figure 8, and the kinetic

DOI: 10.1021/jacs.5b08508
J. Am. Chem. Soc. 2015, 137, 13121−13129

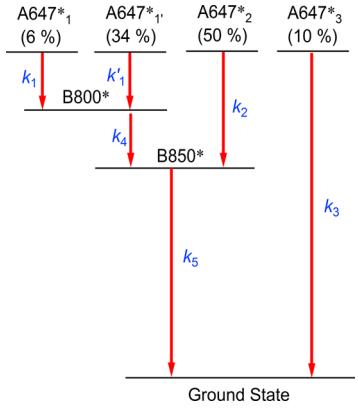

Figure 8. Energy transfer kinetics diagram for LH2−A647 conjugate.

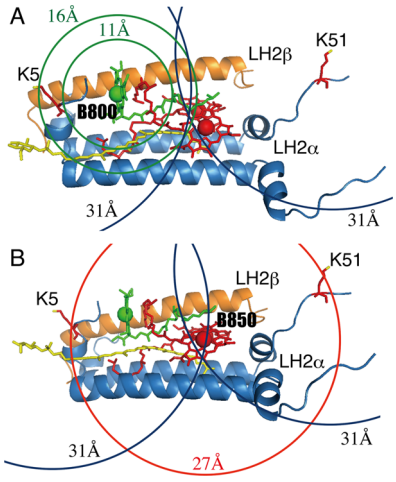

Figure 9. Geometrical description of LH2−A647 consisting of B800, B850, LH2 α- and β-polypeptides. Energy transfer distances from B800 (A) and B850 (B) to A647 estimated by the Förster mechanism are depicted by green (A) and red circles (B). Possible range of A647 attached to K5 and K51 with the linkage moiety was estimated to be 31 Å as fully extended conformation, which is depicted by blue circles. The molecular structure of LH2 was depicted by PyMOL on the basis of the crystallographic structure 1NKZ (PDB).[21]

equations are derived based on this model. The A647* is divided into four independent species. They transfer energy by way of B800 to B850 with short and long time constants (A647*$_1$ and A647*$_{1'}$), directly to B850 (A647*$_2$), or return to the ground state without any energy transfer (A647*$_3$). Six rate constants, k_1, $k_{1'}$−k_5, are required to describe the kinetics, with the values for three of them already known, i.e., k_4^{-1} = 700 fs and $k_3^{-1} = k_5^{-1}$ = 1.2 ns.[22,23,39,40] The TA spectra of the excited states, A647*, B800*, and B850*, were reconstructed by the sum of multiple Gaussian functions. Time evolution of population of each state was obtained by least-squares-fitting of the TA spectra utilizing the reconstructed spectra[43] (details are described in Supporting Information). As a result, the lifetime (intensity ratio) of each A647* was found to be the following: A647*$_1$, 0.44 ps (0.06); A647*$_{1'}$, 4.1 ps (0.34); A647*$_2$, 23 ps (0.50); and A647*$_3$, 1.2 ns (0.10). These values are consistent with those obtained by the global analysis (i.e., 0.26 ps (0.14), 4.3 ps (0.35), 23 ps (0.42), and 1.2 ns (0.09)). The lifetime of 0.26 ps may involve not only the energy transfer but also either ultrafast structural relaxation or solvation dynamics of A647*, because the maximum wavelength of the corresponding DAS was ∼10 nm shorter than those of the ones with longer time constants as mentioned before. Thus, the time constant of 0.44 ps should be closer to the actual value of energy transfer, as the analysis considers the total kinetics. We have also carried out similar analyses assuming that the only component that undergoes energy transfer through B800 is the one with a subpicosecond time constant, although it did not result in a better fit. Thus, it is concluded that the 4 ps component also represents energy transfer from A647 via B800 to B850.

Förster Mechanism. The obtained time constants can be rationalized by Förster mechanism.[30] The estimated donor−acceptor distances (R_{calcd}) and Förster radii (R_0) together with other parameters are summarized in Table 1. The donor−acceptor distances on the basis of Förster mechanism were depicted in the structure of LH2 in Figure 9. The faster rate constants, 440 fs and 4.1 ps, predicted 11 and 16 Å of donor−acceptor distances (Figure 9A). Considering possible areas for A647 with 31 Å radius, which represents fully extended A647 moiety with the linkage from K5 and K51, the A647 linked to K5, thus, can be regarded as the donor for B800, but not that of K51. The time constants could arise from transfer to the closest and the second closest B800 BChls. For B850 as the primary acceptor, however, A647 attached to either K5 or K51 is capable to be the direct donor to B850 as shown in Figure 9B.

The orientation factor, κ^2, is evaluated to be 2/3, as in the case of random orientation toward the acceptors B800 and B850. The flexible and long linkage segment (∼3 nm) for attaching A647 would provide random orientation of A647 and the time constants in the range of subpicoseconds to tens of picoseconds for the energy transfer. Using a rigid and short linker moiety that gives ideal mutual orientation of chromophores would lead to higher efficiency of energy transfer. Thus, we also examined direct attachment of A647 to Lys residues using succinimidyl ester-bearing A647 with a shorter linkage moiety (∼1 nm). However, energy transfer efficiency was decreased to about one-half (data not shown). This result implies that flexible or moderately long linkages enable A647 to approach closer to B800 and B850 through interaction with the hydrophilic regions (N- and C-terminals) or with the outer hydrophobic area of LH2 covered with surfactant molecules. Spectral overlap is also one of the important parameters to increase the efficiency. If the emission band of the attached artificial fluorophore is red-shifted by 50 nm, the energy transfer rate to B800 is expected to be enhanced by 10 times, whereas the effect is less prominent for B850, which has broad and higher exciton bands in the shorter wavelength region.

Biohybrid systems consisting of photosynthetic pigment−protein complexes and artificial fluorophores have been reported.[4−6,8] For Alexa Fluor 660 attached to RC (from *Rhodobacter sphaeroides* mutant) within the Förster energy-transfer distance, the time constant for the fastest energy transfer component was reported to be 40 ps (67.9%).[8] Previous studies using reconstituted LH1-type complexes have demonstrated that various external chromophores attached to LH1-polypeptides exhibit efficient energy transfer from the chromophores to B820 and B875 BChls (∼90%) by Förster mechanism.[4−6] The fastest energy transfer from the attached chromophores to dimeric and oligomeric BChl complexes (B820 and B875) were reported to occur in a time scale of 1−10 ps.[5,6] The time resolution for both experiments are 100−150 fs (fwhm), which is short enough to observe subpicosecond

DOI: 10.1021/jacs.5b08508
J. Am. Chem. Soc. 2015, 137, 13121−13129

Table 1. Estimated Förster Energy-Transfer Parameters for LH2−A647[a]

acceptor	time constant (ps)	k_{et} (s^{-1})	J ($\times 10^{-13}$ cm^6)	R_0 (Å)	R_{calcd} (Å)	fraction of contribution to ET
B800	0.44	2.3×10^{12}	0.7	40	11	0.06
B800	4.1	2.4×10^{11}	0.7	40	16	0.34
B850	23	4.3×10^{10}	3.1	52	27	0.5

[a]The spectral overlap, J (cm^6), was calculated by using PhotochemCad.[44] The orientation term $\kappa^2 = 2/3$ was used. The fluorescence quantum yield of A647 without acceptor, Φ_f, and solvent refractive index, n, were used as 0.33 and 1.333, respectively. The spectral overlap integrals of emission for A647 with B800 and B850 absorption spectra were calculated by using spectra of B800-only (B850-subtracted) and B850-only (B800-subtracted) LH2.

components, if they exist. For the reconstituted LH1 assemblies, the lifetimes of the BChl complexes were significantly short and heterogeneous, i.e., 50 ps (20%) and 600 ps (80%) for B820 and 5−10 ps (25%), 40 ps (60%), and 300 ps (15%) for B875.[5,6] The short lifetime of the final energy acceptor would result in difficulties in precise determination of the energy transfer dynamics and also in their application to an efficient light-energy conversion system.

This work using the LH2 framework indicates that by attachment of appropriate donor fluorophores close to B800, the ultrafast energy transfer cascade can be accomplished, where the natural ultrafast channel B800 → B850 is involved. B850/B800 assemblies in LH2 with the stable and definitive structure provide a faster energy transfer pathway and a longer final exciton lifetime, 1.2 ns, which could be efficiently utilized by the subsequent energy conversion processes. In addition, LH2 is well characterized by various time-resolved spectroscopic data over the past two decades, providing base frameworks for searching and constructing semiartificial light-harvesting devices that work in ultrafast time domains. A combination of such modified LH2 excitonic devices with a photovoltaic LH1-RC will produce highly efficient light-energy conversion systems that afford solar energy in the broad spectrum.

CONCLUSIONS

We demonstrated that the artificial pigment A647 attached to LH2, without affecting inherent functions of LH2, performs efficient energy transfer to B800/B850 inside LH2 in the ultrafast time domain. Femtosecond TA spectroscopy and detailed kinetic analyses revealed that the pathway via B800 is much faster (0.44 and 4.1 ps in 40% contribution) than the pathway of direct transfer to B850 (23 ps in 50% contribution). A647 attached to the N-terminal region of LH2 α-polypeptide, which is closer to B800, most likely contributes to the former pathway. The energy transfer kinetics for LH2−A647 is explainable in terms of Förster mechanism.

The simple strategy of attaching an auxiliary light-harvesting pigment through flexible linkages successfully expanded the available wavelength range to the 620−750 nm region, where LH2 absorbs less photons. Efficient energy transfer, ca. 90%, results from both the ultrafast energy transfer dynamics and from the absence of quenching of A647 through singlet−singlet annihilation due to the absence of dipole and electronic coupling between A647 molecules that are randomly arranged around LH2 scaffold. To develop panchromatic light-harvesting systems using multichromophores,[4] such a flexible linkage of attaching artificial chromophores to LH2 is expected to prevent unfavorable stacking of auxiliary pigments.

The arrangement of A647 around LH2 is heterogeneous and the rate of energy transfer is dispersed in a wide range of time. The challenge is to optimize the orientation of auxiliary pigment through a defined fixation to achieve the fastest energy transfer. Eliminating the 1.2 ns component can achieve 100% efficiency and modification at specific sites would lead to subpicosecond energy transfer. Since A647 is highly hydrophilic,[45] it can directly access to the hydrophilic domains of LH2, and indirectly to the hydrophobic area through assistance of bound surfactant molecules. A promising attempt would be to utilize hydrophobic auxiliary pigments; such pigments can more closely access to the B800/B850 acceptors and provide faster direct transfer to B850, which has not yet been attained with A647. Using a protein scaffold that tightly binds auxiliary pigments would be also a promising approach toward this purpose.[1]

LH2 conjugated with artificial pigments, therefore, will produce a promising motif in the methodology to construct multichromophore devices. This will provide deeper understanding of highly efficient energy transfer processes in natural photosynthetic systems, and clues for construction of highly efficient artificial photosynthetic systems.

MATERIALS AND METHODS

All chemicals and reagents were obtained commercially and used without further purification, unless stated otherwise. LH2 complexes were isolated from membranes of *R. acidophila* strain 10050 and were purified as previously described.[46]

Preparation of LH2−A647. Sulfosuccinimidyl 6-[3′-(2-pyridyldithio]propionamido)hexanoate (sulfo-LC-SPDP, Thermo Scientific) was added to a solution of LH2 dissolved in 50 mM phosphate buffer (pH 7.0) containing 0.1% *N*,*N*-dimethyldodecylamine-*N*-oxide (LDAO) at a ratio of LH2/Sulfo-LC-SPDP = 1/100 (mol/mol) to react for 4 h at 4 °C under darkness. Unreacted Sulfo-LC-SPDP was removed with a Micro Bio-Spin 30 chromatography column (Bio-Rad) to obtain lysine-modified LH2 (LH2-PDP). Subsequent deprotection reaction with dithiothreitol (DTT, LH2/DTT = 1:300 mol ratio) for 1 h at 4 °C under darkness afforded thiol-bearing LH2 (LH2-SH), followed by purification with a PD-10 desalting column (GE Healthcare) by washing with a TL buffer solution (20 mM Tris-HCl, pH 7.0, 0.1 wt % LDAO). Maleimide-C2-Alexa647 (Molecular Probes) was added to a solution of LH2-SH (OD = ca. 50 at 860 nm in TL buffer) at maleimide-C2-Alexa647/LH2 = 50/1 molar ratio to form LH2−A647 conjugate. After incubation at 4 °C overnight under darkness, unreacted dyes were removed with a centrifugation filter [Amicon Ultra 15 (Millipore)] at 3000 rpm with more than 10 times of replacement with a TL buffer solution (pH 7.0) to obtain purified LH2−A647.

Steady-State Fluorescence Spectroscopy. The concentration of LH2 and LH2−A647 in solutions (20 mM Tris-HCl, pH 8.0, containing 0.1 wt % LDAO) for fluorescence measurements was adjusted to an optical density of 0.1 in the B850 absorption band. Steady-state fluorescence spectra were obtained using a spectrometer with a CCD detector as described previously.[47] Excitation spectra were acquired by normalized intensity of incident light with a photodiode sensor. All data were obtained at room temperature. For excitation spectrum, comparisons were not made with the absorption spectrum. Instead, absorptance, $1 - T$, spectrum, where T is the transmittance, to directly compare numbers of input and output photons, was used.

DOI: 10.1021/jacs.5b08508
J. Am. Chem. Soc. 2015, 137, 13121−13129

Absorption spectra were obtained with a Shimadzu UV-1800 spectrophotometer at ambient temperature.

Transient Absorption Spectroscopy. The experimental set up for transient absorption (TA) measurements is similar to those utilized in previous studies.[48,49] The femtosecond Ti:sapphire laser (Tsunami, Spectra-Physics) was pumped by the SHG of a cw Nd^{3+}:YVO_4 laser (Millennia V, Spectra-Physics). The output was regeneratively amplified with 1 kHz repetition rate (Spitfire, Spectra-Physics) and the amplified pulse had an energy of 1 mJ/pulse and pulse duration of 85 fs fwhm with a repetition rate of 1 kHz. The amplified pulse was divided into two pulses with a 50/50% ND filter and guided into a pair of noncollinear optical parametric amplifier systems (TOPAS-white, Light-Conversion). The wavelength of the output was computer controlled. Quarter waveplate was used to obtain circular polarization of the pump pulse to avoid the effect of polarization anisotropy.

Self-diffraction frequency-resolved optical gating (SD-FROG) measurement was carried out to obtain the autocorrelation trace of the pump pulse. The pulse duration was optimized to be the shortest at the sample position by a pulse compressor inside TOPAS-white with two wedged fused silica plates. The output of TOPAS-white with its spectrum centered at ∼650 nm was utilized to excite the absorption band of A647 conjugated to LH2 that peaks at 653 nm. The bandwidth of the pulse was nearly 90 nm and the pulse duration was ∼17 fs with energy of 10.5 nJ. Meanwhile, by focusing the output of the other TOPAS-white (center wavelength, 1000 nm) into a rotating CaF_2 window (optical path, 2 mm), white-light supercontinuum was generated.

The signal and the reference pulses in the wavelength range of 400−950 nm were detected with two pairs of spectrometer and multichannel photodiode array system (PMA-10, Hamamatsu) and the data were sent to a personal computer. A cross-correlation trace between the pump pulse and the white-light supercontinuum was obtained by an optical Kerr effect (OKE) measurement. Group velocity dispersion curve of the experimental setup was obtained by least-squares-fitting of the cross-correlation trace and the TA signals were calibrated based on this data. Global analysis utilizing multiple exponential functions was carried out to elucidate the transient kinetics. The amplitude of each component (pre-exponential factor) was a complete variable at each wavelength, while the time constants were linked to obtain the same set of values at every wavelengths. The differential absorbance at each wavelength was assorted according to the amplitude ratio of the components and the decay associated spectra (DAS) were obtained.

■ ASSOCIATED CONTENT

Supporting Information

The Supporting Information is available free of charge on the ACS Publications website at DOI: 10.1021/jacs.5b08508.

Additional experimental methods and data (PDF)

■ AUTHOR INFORMATION

Corresponding Authors

*takedewa@nitech.ac.jp

*ynagasa@fc.ritsumei.ac.jp

Present Address

⊗Department of Applied Chemistry, College of Life Science, Ritsumeikan University, 1-1-1 Noji-Higashi, Kusatsu, Shiga 525-8577, Japan.

Notes

The authors declare no competing financial interest.

■ ACKNOWLEDGMENTS

This work was partially supported by PRESTO (Japan Science and Technology Agency, JST) and also partially supported by a Grant-in-Aid for Scientific Research on Innovative Areas "Photosynergetics" (No. 2606, 26107002) from MEXT, Japan. T.D. and T.N. thank Tatematsu, Takahashi, and Hibi Foundations for funding. M.N. and T.D. also thank AOARD for funding. The authors thank Prof. Shinya Kitagawa at Nagoya Institute of Technology for helpful discussion and comments on mass spectroscopy. The authors thank also Dr. Hisanori Yamakawa (Graduate School of Bioagricultural Sciences, Nagoya University) for the measurements of fluorescence lifetimes. The authors are grateful to Prof. Richard J. Cogdell and Dr. Alastair T. Gardiner (University of Glasgow) for the gift of photosynthetic bacterial culture.

■ REFERENCES

(1) Noriega, R.; Finley, D. T.; Haberstroh, J.; Geissler, P. L.; Francis, M. B.; Ginsberg, N. S. *J. Phys. Chem. B* **2015**, *119*, 6963.

(2) Zeng, X.-L.; Tang, K.; Zhou, N.; Zhou, M.; Hou, H. J. M.; Scheer, H.; Zhao, K.-H.; Noy, D. *J. Am. Chem. Soc.* **2013**, *135*, 13479.

(3) Adams, P. G.; Collins, A. M.; Sahin, T.; Subramanian, V.; Urban, V. S.; Vairaprakash, P.; Tian, Y.; Evans, D. G.; Shreve, A. P.; Montaño, G. A. *Nano Lett.* **2015**, *15*, 2422.

(4) Harris, M. A.; Jiang, J.; Niedzwiedzki, D. M.; Jiao, J.; Taniguchi, M.; Kirmaier, C.; Loach, P. A.; Bocian, D. F.; Lindsey, J. S.; Holten, D.; Parkes-Loach, P. S. *Photosynth. Res.* **2014**, *121*, 35.

(5) Harris, M. A.; Parkes-Loach, P. S.; Springer, J. W.; Jiang, J.; Martin, E. C.; Qian, P.; Jiao, J.; Niedzwiedzki, D. M.; Kirmaier, C.; Olsen, J. D.; Bocian, D. F.; Holten, D.; Hunter, C. N.; Lindsey, J. S.; Loach, P. A. *Chem. Sci.* **2013**, *4*, 3924.

(6) Springer, J. W.; Parkes-Loach, P. S.; Reddy, K. R.; Krayer, M.; Jiao, J.; Lee, G. M.; Niedzwiedzki, D. M.; Harris, M. A.; Kirmaier, C.; Bocian, D. F.; Lindsey, J. S.; Holten, D.; Loach, P. A. *J. Am. Chem. Soc.* **2012**, *134*, 4589.

(7) Buczynska, D.; Bujak, Ł.; Loi, M. A.; Brotosudarmo, T. H. P.; Cogdell, R.; Mackowski, S. *Appl. Phys. Lett.* **2012**, *101*, 173703.

(8) Dutta, P. K.; Lin, S.; Loskutov, A.; Levenberg, S.; Jun, D.; Saer, R.; Beatty, J. T.; Liu, Y.; Yan, H.; Woodbury, N. W. *J. Am. Chem. Soc.* **2014**, *136*, 4599.

(9) Milano, F.; Tangorra, R. R.; Hassan Omar, O.; Ragni, R.; Operamolla, A.; Agostiano, A.; Farinola, G. M.; Trotta, M. *Angew. Chem., Int. Ed.* **2012**, *51*, 11019.

(10) Nabiev, I.; Rakovich, A.; Sukhanova, A.; Lukashev, E.; Zagidullin, V.; Pachenko, V.; Rakovich, Y. P.; Donegan, J. F.; Rubin, A. B.; Govorov, A. O. *Angew. Chem., Int. Ed.* **2010**, *49*, 7217.

(11) Nakamura, A.; Mizoguchi, S.; Yoshida, E.; Kato, Y.; Watanabe, T. *Chem. Lett.* **2005**, *34*, 1472.

(12) *Light-Harvesting Antennas in Photosynthesis*; Green, B. R., Parson, W. W., Eds.; Kluwer Academic Publishers: Dordrecht, 2003.

(13) Cogdell, R. J.; Lindsay, J. G. *New Phytol.* **2000**, *145*, 167.

(14) Blankenship, R. E. *Molecular Mechanisms of Photosynthesis*; Wiley Blackwell: Oxford, U.K., 2014.

(15) Sundström, V.; Pullerits, T.; van Grondelle, R. *J. Phys. Chem. B* **1999**, *103*, 2327.

(16) van Grondelle, R.; Novoderezhkina, V. I. *Phys. Chem. Chem. Phys.* **2006**, *8*, 793.

(17) Cheng, Y.-C.; Fleming, G. R. *Annu. Rev. Phys. Chem.* **2009**, *60*, 241.

(18) Scholes, G. D.; Fleming, G. R.; Olaya-Castro, A.; van Grondelle, R. *Nat. Chem.* **2011**, *3*, 763.

(19) McDermott, G.; Prince, S. M.; Freer, A. A.; Hawthornthwaite-Lawless, A. M.; Papiz, M. Z.; Cogdell, R. J.; Isaacs, N. W. *Nature* **1995**, *374*, 517.

(20) Koepke, J.; Hu, X.; Muenke, C.; Schulten, K.; Michel, H. *Structure* **1996**, *4*, 581.

(21) Papiz, M. Z.; Prince, S. M.; Howard, T.; Cogdell, R. J.; Isaacs, N. W. *J. Mol. Biol.* **2003**, *326*, 1523.

(22) Hess, S.; Feldchtein, F.; Babin, A.; Nurgaleev, I.; Pullerits, T.; Sergeev, A.; Sundström, V. *Chem. Phys. Lett.* **1993**, *216*, 247.

(23) Joo, T.; Jia, Y.; Yu, J.-Y.; Jonas, D. M.; Fleming, G. R. *J. Phys. Chem.* **1996**, *100*, 2399.

DOI: 10.1021/jacs.5b08508
J. Am. Chem. Soc. 2015, 137, 13121−13129

(24) Cong, H.; Niedzwiedzki, D. M.; Gibson, G. N.; LaFountain, A. M.; Kelsh, R. M.; Gardiner, A. T.; Cogdell, R. J.; Frank, H. A. *J. Phys. Chem. B* **2008**, *112*, 10689.
(25) Polívka, T.; Zigmantas, D.; Herek, J. L.; He, Z.; Pascher, T.; Pullerits, T.; Cogdell, R. J.; Frank, H. A.; Sundström, V. *J. Phys. Chem. B* **2002**, *106*, 11016.
(26) Polli, D.; Cerullo, G.; Lanzani, G.; De Silvestri, S.; Hashimoto, H.; Cogdell, R. J. *Biophys. J.* **2006**, *90*, 2486.
(27) Roszak, A. W.; Howard, T. D.; Southall, J.; Gardiner, A. T.; Law, C. J.; Isaacs, N. W.; Cogdell, R. J. *Science* **2003**, *302*, 1969.
(28) Fleming, G. R.; van Grondelle, R. *Curr. Opin. Struct. Biol.* **1997**, *7*, 738.
(29) Scholes, G. D. *J. Phys. Chem. Lett.* **2010**, *1*, 2.
(30) Hu, X.; Ritz, T.; Damjanovic, A.; Schulten, K. *J. Phys. Chem. B* **1997**, *101*, 3854.
(31) Fraser, N. J.; Dominy, P. J.; Ücker, B.; Simonin, I.; Scheer, H.; Cogdell, R. J. *Biochemistry* **1999**, *38*, 9684.
(32) Herek, J. L.; Fraser, N. J.; Pullerits, T.; Martinsson, P.; Polívka, T.; Scheer, H.; Cogdell, R. J.; Sundström, V. *Biophys. J.* **2000**, *78*, 2590.
(33) Gall, A.; Robert, B.; Cogdell, R. J.; Bellissent-Funel, M.-C.; Fraser, N. J. *FEBS Lett.* **2001**, *491*, 143.
(34) Förster, T. *Discuss. Faraday Soc.* **1959**, *27*, 7.
(35) Koolhaas, M. H. C.; Frese, R. N.; Fowler, G. J. S.; Bibby, T. S.; Georgakopoulou, S.; van der Zwan, G.; Hunter, C. N.; van Grondelle, R. *Biochemistry* **1998**, *37*, 4693.
(36) Mukai, K.; Abe, S.; Sumi, H. *J. Phys. Chem. B* **1999**, *103*, 6096.
(37) Cogdell, R. J.; Gall, A.; Köhler, J. *Q. Rev. Biophys.* **2006**, *39*, 227.
(38) Ma, Y.-Z.; Cogdell, R. J.; Gillbro, T. *J. Phys. Chem. B* **1997**, *101*, 1087.
(39) Chen, X.-H.; Zhang, L.; Weng, Y.-X.; Du, L.-C.; Ye, M.-P.; Yang, G.-Z.; Fujii, R.; Rondonuwu, F. S.; Koyama, Y.; Wu, Y.-S.; Zhang, J. P. *Biophys. J.* **2005**, *88*, 4262.
(40) Monshouwer, R.; Abrahamsson, M.; van Mourik, F.; van Grondelle, R. *J. Phys. Chem. B* **1997**, *101*, 7241.
(41) Kosumi, D.; Nakagawa, K.; Sakai, S.; Nagaoka, Y.; Maruta, S.; Sugisaki, M.; Dewa, T.; Nango, M.; Hashimoto, H. *J. Chem. Phys.* **2013**, *139*, 034311.
(42) Desamero, R. Z. B.; Chynwat, V.; van der Hoef, I.; Jansen, F. J.; Lugtenburg, J.; Gosztola, D.; Wasielewski, M. R.; Cua, A.; Bocian, D. F.; Frank, H. A. *J. Phys. Chem. B* **1998**, *102*, 8151.
(43) Ishibashi, Y.; Katayama, T.; Saito, H.; Yamanaka, K.-i.; Goto, Y.; Tani, T.; Okada, T.; Inagaki, S.; Miyasaka, H. *J. Phys. Chem. C* **2014**, *118*, 9419.
(44) Dixon, J. M.; Taniguchi, M.; Lindsey, J. S. *Photochem. Photobiol.* **2005**, *81*, 212.
(45) Hughes, L. D.; Rawle, R. J.; Boxer, S. G. *PLoS One* **2014**, *9*, e87649.
(46) Papiz, M. Z.; Hawthornthwaite, A. M.; Cogdell, R. J.; Woolley, K. J.; Wightman, P. A.; Ferguson, L. A.; Lindsay, J. G. *J. Mol. Biol.* **1989**, *209*, 833.
(47) Sumino, A.; Dewa, T.; Noji, T.; Nakano, Y.; Watanabe, N.; Hildner, R.; Bösch, N.; Köhler, J.; Nango, M. *J. Phys. Chem. B* **2013**, *117*, 10395.
(48) Nagasawa, Y.; Fujita, K.; Katayama, T.; Ishibashi, Y.; Miyasaka, H.; Takabe, T.; Nagao, S.; Hirota, S. *Phys. Chem. Chem. Phys.* **2010**, *12*, 6067.
(49) Ishibashi, Y.; Umesato, T.; Kobatake, S.; Irie, M.; Miyasaka, H. *J. Phys. Chem. C* **2012**, *116*, 4862.

DOI: 10.1021/jacs.5b08508
J. Am. Chem. Soc. 2015, 137, 13121−13129